Food Chemistry: X 14 (2022) 100338

Contents lists available at ScienceDirect

Food Chemistry: X

journal homepage: www.sciencedirect.com/journal/food-chemistry-x

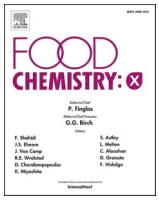

Research on physicochemical properties, microscopic characterization and detection of different freezing-damaged corn seeds

Jun Zhang, Zhiying Wang, Maozhen Qu, Fang Cheng *

College of Biosystems Engineering and Food Science, Zhejiang University, Hangzhou 310058, China

ARTICLE INFO

Keywords:
Corn (*Zea mays* L.)
Freezing damage
Germination
Enzymes activity
Microscopic observation
Classification
Near-infrared spectroscopy

ABSTRACT

Seed freezing damage is an agricultural disaster. To explore how frostbite affects the growth and development of corn seeds, the germination conditions, and the biological indicators including the activities of related enzymes (SOD, POD, CAT, and AMS) of different frozen corn seeds (normal, −10 °C,10 h, and −20 °C,10 h) were measured. The texture of seed coat and the cell structure of seed embryo were observed by scanning electron microscope and transmission electron microscope respectively. The texture and cell structural changes reflect the influence of frostbite on corn seeds. To propose a quick, accurate and non-destructive method to identify the freezing-damaged corn seeds, near-infrared spectroscopy was used the identify the different frozen corn seeds. Different pretreatments, feature extraction methods and modeling methods were applied, result showed that in the case of standard normal variation pretreatment combined with principal component analysis feature extraction method and K-nearest neighbor model, 99.4 % and 100 % classification results of the training set and testing set were obtained respectively.

1. Introduction

As one of the three major food crops, corn (*Zea mays* L.) is widely used in the food and feeding field (Ambrose, Kandpal, Kim, Lee, & Cho, 2016). China, as the world's second-largest corn producing and consuming country, the yield of corn seeds in 2020 is 26.067 billion kg (stats.gov.cn, 2021). China's Hexi Corridor area (including Gansu Province and other regions) is the main seed production base for corn, which bears more than 70 % of the country's seed production needs (Zhang, Dai, & Cheng, 2019). As we all know, the quality of seeds has a great relationship with whether the seeds can grow normally and obtain high yields. However, due to the geographical location, the weather in these production areas is relatively cold at harvest time (October or November), and sometimes frost occurs, causing a great impact on the seed growth process. Thus, seed freezing damage is an agricultural disaster (Akinyosoye, Adetumbi, Amusa, Olowolafe, & Olasoji, 2014; Zhang, et al., 2019; Zhang, Dai, & Cheng, 2021a).

Regarding the research on corn seed freezing damage, related scholars have studied the effects of corn seed maturity, moisture content, freezing temperature and duration on seed germination (DeVries, Goggi, & Moore, 2007; Woltz, Egli, & TeKrony, 2005; Woltz, TeKrony, & Egli, 2006). Woltz et al. (2006) reported that when the most immature seeds frozen with the seed moisture content (SMC) of 40 %, severe reductions in seed germination and vigor occurred. The effect was reduced as seed developed for all hybrids when the SMC is less than 30 % (Woltz, et al., 2006). Woltz et al. (2005) studied the freezing point temperature harvested at various stages of development of corn seeds (seed, embryo, and endosperm tissue). As seeds matured with the SMC less than 40 %, the embryo tissue had higher freezing at warmer temperatures (−4.5 °C) than the endosperm (−9.2 °C) (Woltz, et al., 2005).

After the freezing damage occurs, the viability of the seeds will reduce. At present, the traditional method of determining seed viability still relies on manual testing, and the test is a professional and destructive work (Akinyosoye, et al., 2014). Thus, it is necessary to propose a quick, accurate and non-destructive method to identify the freezing-damaged corn seeds.

Near infrared spectroscopy (NIRS) technology is a rapid nondestructive testing technology, and it has many applications in the detection of corn seeds (Armstrong, 2007; Da Conceição, et al., 2021; Gustin, et al., 2013; Lin, Yu, Li, & Qin, 2018; Qiao, et al., 2022), such as the variety classification (Cui, et al., 2018; Yang, Hong, You, & Cheng, 2015; Zhang, Dai, & Cheng, 2021b), viability (Qiu, et al., 2018), the internal constituents (Egesel, Kahrıman, Ekinci, Kavdır, & Büyükcan, 2016; Zhong & Qin, 2016). There are also researches using spectral technology

* Corresponding author at: Zhejiang University, 866 Yuhangtang Road, Hangzhou 310058, China.
E-mail address: fcheng@zju.edu.cn (F. Cheng).

https://doi.org/10.1016/j.fochx.2022.100338
Received 14 November 2021; Received in revised form 19 April 2022; Accepted 18 May 2022
Available online 21 May 2022

combined with different algorithms to realize the classification of different frozen corn seeds. Jia et al. (2016) used NIRS and chemometrics to study the feasibility of analyzing frost-damaged and non-viable maize seeds. The model obtained the highest average accuracy of 97 % (Jia, et al., 2016). Zhang et al. used hyperspectral imaging technology combined with different algorithms to realize the classification of different freezing-damaged corn seeds. The conductivity of corn seeds in three different conditions was measured. Results showed that the established model can obtain the classification accuracy of more than 90 % (Zhang, et al., 2019). In 2021, Zhang et al. combined hyperspectral imaging technology with deep learning method to identify the freezing-damaged corn seeds. Results showed that deep convolutional neural network model has the most satisfactory result for four and five category classification (Zhang, et al., 2021a).

The current studies have explored the influencing factors of seed frostbite, realizing the classification of freezing-damaged corn seeds, and achieving good classification results. However, it is not clear how frostbite affects the growth and development of corn seeds, how frostbite affects different parts of the corn seeds, the research on the micro-observation of corn seeds after frostbite are worth exploring. When the seed suffered from frost, there may be some changes in the surface of the seed coat, and the embryo that grows into a seedling will have the greatest impact. Therefore, the research objectives of this study were to: Explore how frostbite affects the growth and development of corn seeds by determining the germination rate, antioxidant enzyme activity and other physical and chemical indicators of the seeds under different frostbite environments; Observe the changes of seed coat by scanning electron microscope (SEM), and observe changes in the cell structure of embryos by transmission electron microscope (TEM), to explain the micro-mechanism of seed frostbite based on these changes; Collect the near-infrared spectroscopy data of the corn seeds, to achieve a wonderful classification performance.

2. Materials and methods

2.1. Samples

The fresh corn seeds (Weike702) were collected from the Gansu Dunhuang Seed Group Co., ltd. (Jiuquan, Gansu Province, China) with the temperature of about 13 °C, and an original moisture content of about 28 % (wet basis) in October 2020. The seeds were placed in a constant temperature refrigerator (Shanghai Lanhao Instrument &Equipment CO.,ltd, Shanghai, China) with the freezing temperatures of −10 °C and −20 °C for 10 h to obtain different freezing-damaged corn seeds (Zhang, et al., 2021a; Zheng, 2010). Then, the seeds were stored at room temperature and the seed moisture content was naturally dropped to about 13 % (wet basis) for germination tests, enzyme activity test, SEM and TEM observation and near infrared spectra data acquisition. Thus, there is no effect of drying method on the microstructure. The moisture content test was conducted according to the China standard GB/T3543.6–1995.

2.2. Germination test

The germination test was conducted according to the China standard GB/T3543.4–1995. Fifty intact corn seeds of each treatment were selected and soaked for 12 h, then the seeds were placed in an artificial climate incubator (Ningbo Jiangnan Instrument Factory, Ningbo, China) with the temperature of 25 °C, and the relative humidity of 75 %. The germination rate of the corn seeds in Day 4 and Day 7 were calculated according to equation (1):

$$GR = 100\ \% \times GN / TN \quad (1)$$

where GR is the germination rate of the corn seeds; GN is the number of germinated seeds; TN is the total of the corn seeds.

2.3. Biological indicators

The activities of the indicators including superoxide dismutase (SOD), peroxidase (POD), catalase (CAT), α-amylase (AMS) were determined using commercially available assay kits (A001-1 for SOD, A084-3–1 for POD, A007-1 for CAT, C016-1–1 for AMS; Nanjing Jiancheng Bioengineering Institute, Jiangsu, China) following the manufacturer's instructions (Lin, et al., 2020). The optical density (OD) values of each reaction mixture were measured by Ultraviolet and Visible Spectrophotometer (UV-2000, UNICO (Shanghai) Instrument Co., ltd., China).

SOD activity was obtained by measuring the change of absorbance at 550 nm. One unit of SOD activity was defined as the amount of enzyme required to cause 50 % SOD inhibition per mg of protein in 1 ml of the reaction solution (Li, et al., 2013).

POD activity was obtained by measuring the change of absorbance at 420 nm. One unit of POD activity was defined as the amount of enzyme that catalyzes 1 μg of substrate per minute per mg protein (Li, et al., 2013).

CAT activity was obtained by measuring the change of absorbance at 405 nm. One unit of CAT activity was defined as the amount of decomposed 1 μmol of H_2O_2 per second per mg protein (Li, et al., 2013).

AMS activity was obtained by measuring the change of absorbance at 660 nm. One unit of AMS activity was defined as: each mg of protein in the tissue reacted with the substrate for 30 min, and hydrolyzed 10 mg of starch (Rajput, et al., 2013).

2.4. SEM and TEM observation

The sample preparation was under the guidance of Bio-ultrastructure analysis Laboratory of Analysis center of Agrobiology and environmental sciences, Zhejiang University. The seed coats in the central embryo part of each treatment were selected for SEM observation. The seed embryos of each treatment were selected for TEM observation. In order to better understand the effect of freezing damage on the seed coat and seed embryo cells, a series of pre-observation processing steps were conducted on the selected samples to be suitable for observing the relevant microscopic changes (Liu, et al., 2022; Lu, et al., 2019).

Seed coat samples were fixed overnight at 4 °C in 0.1 M PBS buffer containing 2.5 % glutaraldehyde (v/v) and postfixed in 1 % OsO4 in the same buffer for 2 h. The samples were then dehydrated through a graded ethanol series [30, 50, 70, 80, 90 and 95 % (v/v in ddH_2O); 15 min at each concentration] followed by a 100 % ethanol for 20 min. After dehydration, the samples were dried and sprayed with gold to enhance the conductivity of the sample surface. the micro-morphology of the seed coats was observed with an accelerating voltage of 30 kV using the scanning electron microscopy (Hitachi SU-8010, Hitachi, Japan).

Seed embryo samples were firstly soaked in a 4 % paraformaldehyde (v/v) for 30 min, and then fixed overnight at 4 °C in 0.1 M PBS buffer containing 5 % glutaraldehyde, 1 % Triton X-100 (v/v) and post-fixed in 1 % OsO4 in the same buffer for 2 h. The samples were then dehydrated through a graded ethanol series [30, 50, 70 and 80 % (v/v in ddH_2O); 15 min at each concentration] followed by a graded acetone series [90 and 95 % (v/v in ethanol); 15 min at each concentration], and followed by Spurr resin:acetone series (1:1 and 3:1; 1 h and 3 h at each concentration) and embedded in 100 % Spurr resin. The sections (60–80 nm) of the samples were obtained with an ultramicrotome and stained after heating at 75. The cell structure of the embryo was observed using the transmission electron microscopy (Hitachi H-7650, Hitachi, Japan).

2.6. Near infrared spectra data acquisition and processing

2.6.1. Data acquisition

In this study, N-500 Fourier Transform Near-Infrared Spectrometer System (BUCHI Labortechnik AG, Switzerland) was used to collect the near-infrared spectroscopy data. The software NIRWare was used to set

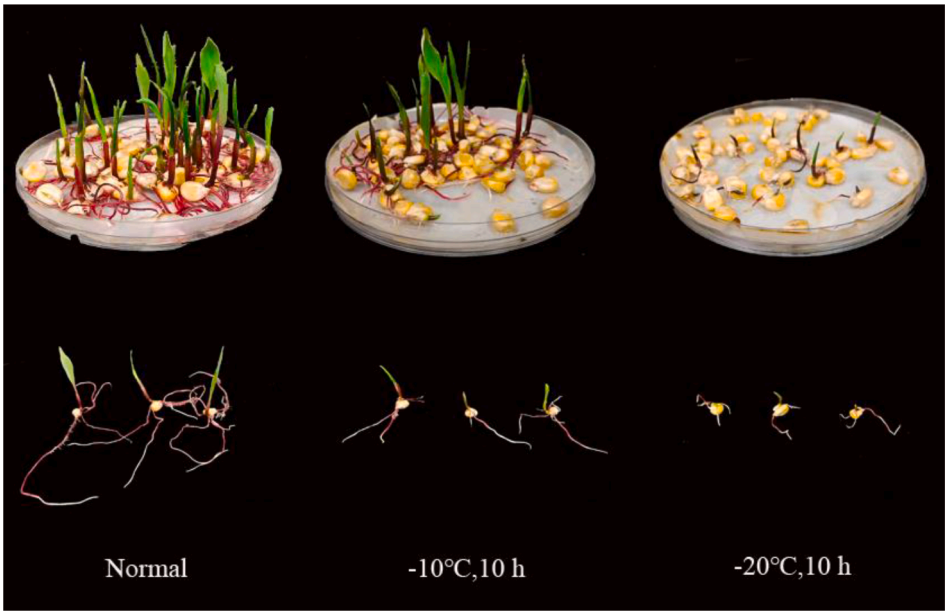

Fig. 1. The growth and development of the seeds on Day 7 under each treatment.

the collecting parameters. The full wavenumber range of the collected spectra was 4000–10000 cm^{-1}, and the collecting interval was 4 cm^{-1}, the scanning times was set to 16, a total of 1501 points were collected, and the averaging times of the spectra was set to 3. 30 corn seeds (about 10.70 g) of each frozen condition were placed in a cuvette at a time, and then, the XL accessory of the solid sample cell was used to collect an averaged near-infrared spectral data in the diffuse reflection mode. In this process, 90 spectral data of each treatment were collected respectively for classification, and a total of 270 spectral data were obtained. The data set was randomly divided according to the ratio of training set and testing set 2:1 for modeling and verification. There was no difference between them. In the end, the number of samples for training set was 180, and the number of samples for testing set was 90.

2.6.2. Data processing

2.6.2.1. Spectral pretreatment methods. To obtain reliable, accurate and stable calibration models, the use of spectral pretreatment methods is needed. The pretreatments have many advantages, such as removing the scatter effect eliminating spectral errors, improving the signal-to-noise ratio. Different pretreatments can bring different effect. In this study, no pretreatment (none), standard normal variation (SNV) and five points and three times smoothing (5–3 smoothing) pretreatment methods were applied (Chen, Song, Tang, Feng, & Lin, 2013; Liu, Sun, & Zeng, 2014). The spectra were preprocessed by MATLAB R2019b (The MathWorks, Natick, MA, USA).

2.6.2.2. Feature extraction method. NIR spectroscopy provides complex structural information. When using the full wavenumber for analysis, problems of data redundancy and long calculation time may arise. In order to improve the efficiency, it is necessary to use the feature extraction method. In this study, the successive projection algorithm (SPA), and principal component analysis (PCA) were applied to obtain important wavenumbers (Candolfi, De Maesschalck, Jouan-Rimbaud, Hailey, & Massart, 1999; Soares, Gomes, Araujo, Filho, & Galvão, 2013; Wold, Esbensen, & Geladi, 1987). The feature wavenumbers were extracted by MATLAB R2019b (The MathWorks, Natick, MA, USA).

2.6.2.3. The classification methods. In traditional spectral data analysis, some pattern recognition methods such as K-nearest neighbor (KNN), support vector machine (SVM) et al. are widely used in data classification. In this study, KNN and SVM models were established for classification of different freezing-damaged corn seeds (Burges, 1998; Mavroforakis & Theodoridis, 2006; Riba Ruiz, Canals, & Cantero Gomez, 2012). The data were classified by MATLAB R2019b (The MathWorks, Natick, MA, USA).

2.6.2.3. The evaluation index of the results. To evaluate the classification performance of the models, the accuracy is applied to evaluate the model performance according to equation (2). It refers to the ratio of the number of correctly classified samples to the total number of all samples. In addition, the confusion matrix of the optimal results is also generated for analysis (de Sousa Fernandes, et al., 2019; Santos, Morais, Nascimento, Araujo, & Lima, 2017). The confusion matrix is a way for accuracy evaluation. After the samples are classified, we can clearly see the classification results of each category samples and the number of samples classified into each category in the form of confusion matrix.

$$\text{Accuracy} = 100\ \% \times A / T \tag{2}$$

A refers to the number of samples that are correctly classified; T refers to the number of samples used for classification.

2.7. Statistical analysis

In this paper, variance analysis (ANOVA) and the significance analysis was applied to analyze the data by Duncan's multiple range tests. Statistical analysis was performed by the software Statistical Package for Social Sciences (SPSS for Windows, SPSS Inc., Chicago, IL, USA). Data were presented as means ± standard deviation and a probability value of P less than 0.05 was considered significant.

3. Results and discussions

3.1. Germination

The germination results of the corn seeds on Day 4 and Day 7 of each treatment are shown in Table A.1. It can be seen that the deeper the degree of frostbite, the lower the germination rate of corn seeds. After four days of germination and cultivation, most of the seeds can germinate under normal conditions. On day 7, the germination of seeds in

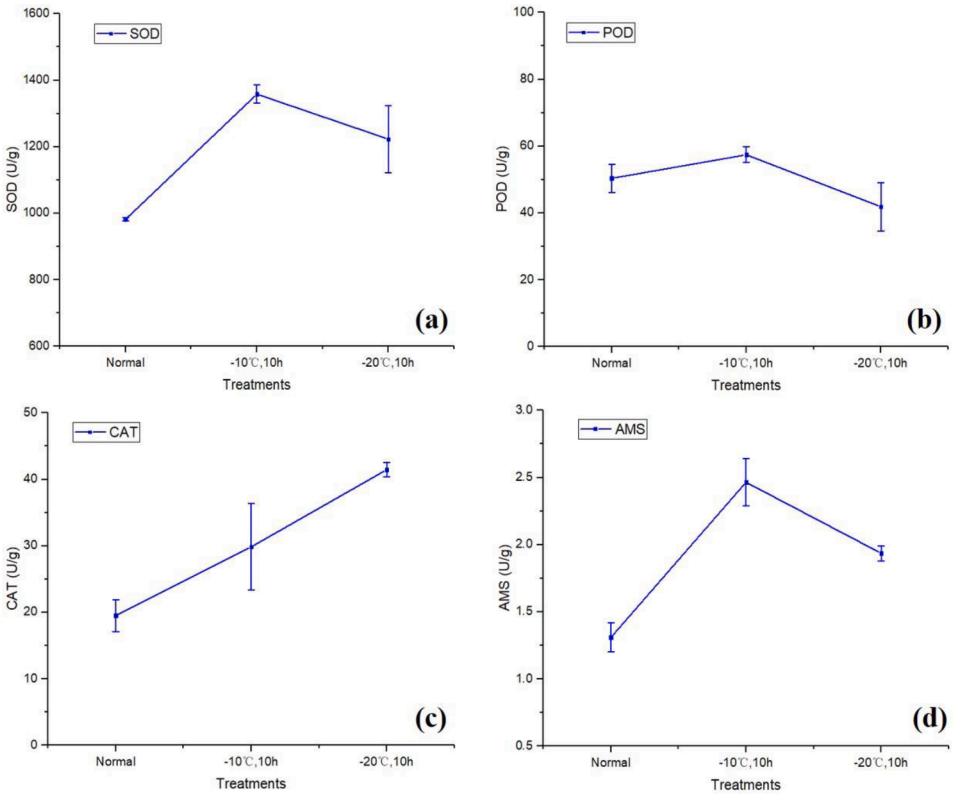

Fig. 2. The changing trend of the enzyme activity of (a) SOD, (b) POD, (c) CAT and (d) AMS under each treatment.

each treatment has increased, and the germination rate of normal seeds is the highest, reaching 88 %. The germination rate of seeds under −10 °C,10 h and −20 °C,10 h frozen conditions are 42 % and 10 % respectively.

Fig. 1 shows the growth and development of the seeds on day 7 under three treatments, and three representative seeds were selected from each treatment for comparison. It can be seen from the figure that the germination condition of the seeds under normal treatment is better than the other two conditions. Under normal treatment, most of the corn seeds grow leaves, and the length of the main root is the longest, and the number of roots is the largest; As for the corn seeds in the case of −10 °C,10 h, a few of corn seeds grow leaves, and the length of the main root is short, with only 2–4 roots growing. As for the corn seeds in the case of −20 °C,10 h, the length of the buds is very short, with no leaves growing and the root length is very short. Due to the influence of low temperature, it has a serious impact on the embryo of the seed, resulting in the corn seeds cannot normally grow into seedlings in the later period.

3.2. Biological indicators

Table A.2 and Fig. 2 show the enzyme activity results of SOD, POD, CAT and AMS. According to the results, it can be seen that the activity results of SOD, CAT and AMS are the lowest under normal conditions, with the activity of 981.492 U/g, 19.507 U/g, and 1.310 U/g respectively; The activity changes of SOD, POD and AMS showed a trend of first increasing and then decreasing, reaching the maximum at −10 °C, 10 h, which were 1358.467 U/g, 57.407 U/g, and 2.466 U/g, respectively; The activity of CAT showed a gradually increasing trend, reaching the maximum at −20℃,10 h, with the activity of 41.474 U/g; Although the change of POD activity showed a trend of increasing first and then decreasing, a relatively low activity was obtained at −20 °C for 10 h. It can be seen that the activity of POD under two freezing conditions (−10 °C,10 h and −20 °C,10 h) is not significantly different from that under normal conditions (P greater than 0.05). The activities of other enzymes showed high significance (P less than 0.05).

SOD, POD and CAT are major antioxidant enzymes in plants, which could remove excess free radicals in plants, effectively inhibit the damage of reactive oxygen-free radicals to the matrix, and thus improve resistance in plants towards stress resistance. Under low temperature stress, the reactive oxygen species scavenging system in maize is changed, which destroys the balance between reactive oxygen species production and scavenging, which adversely affects the growth and development of maize (Nan, 2010). The increase of SOD, POD and CAT activity can scavenge active oxygen free radicals to protect seed cells from active oxygen damage, and ultimately maintain the stability of the membrane system to enhance the ability to resist freezing damage (Nan, 2010).

From the results, it can be seen that SOD and POD increased till −10 °C, then decreased at −20 °C. As the first line of defense in the antioxidant system, the main function of SOD is to convert two O_2^- radicals into H_2O2 and O_2 (Sun, Zhou, Sun, & Jin, 2007). POD is the main H_2O_2 scavenging enzyme to remove the reactive oxygen species. However, with the deepening of low temperature, especially under the frozen condition of 20 °C for 10 h, the stress damage continued to accumulate, and the metabolism of corn seed may be further deregulated (Nan, 2010). The amount of reactive oxygen species produced is less increased, resulting in the activity of SOD and POD may be decreased to an extent. The main function of CAT is to reduce the content of H_2O_2, which is mainly achieved by decomposing H_2O_2 into H_2O and O_2 (Gratão, Polle, Lea, & Azevedo, 2005). There are many ways that lead to the produce of H_2O_2, resulting in the activity of CAT increased even at −20 °C. Therefore, it is proved that the various enzymes protecting the enzyme system in the process of plant anti-low temperature work in coordination with each other, rather than relying only on the activity change of a certain enzyme. The increase in AMS activity can regulate cell permeability to resist low temperature stress. But why the enzyme activity becomes smaller at −20 °C, this may be related to the severely damaged in the cell structure, resulting in the enzyme activity

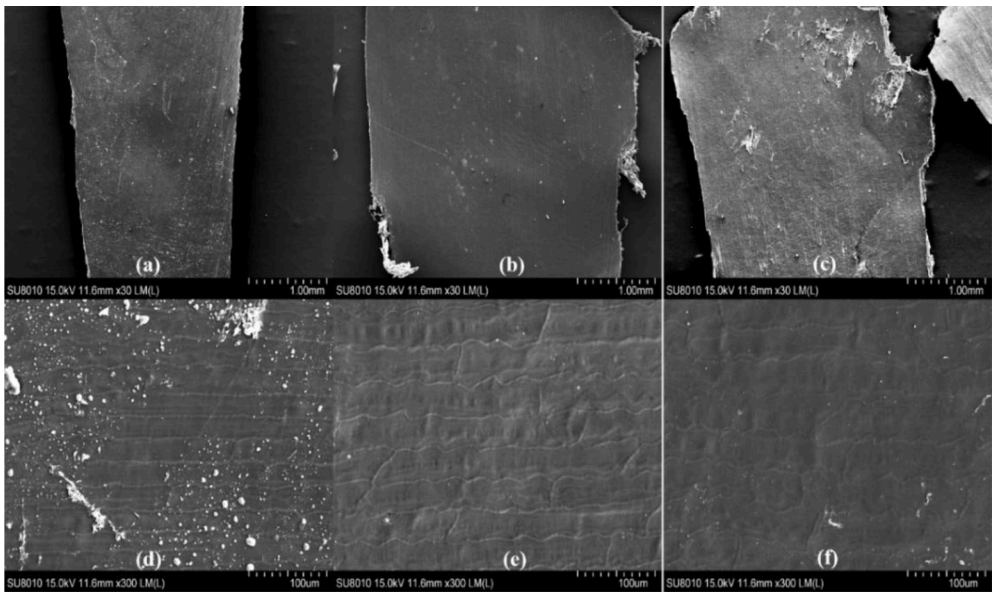

Fig. 3. The SEM images of the seed coat under each treatment. (a) the seed coat of normal seeds (×30); (b) the seed coat of seeds with −10 °C for 10 h (×30); (c) the seed coat of seeds with −20 °C for 10 h (×30); (d) the seed coat of normal seeds (×300); (e) the seed coat of seeds with −10 °C for 10 h (×300); (f) the seed coat of seeds with −20 °C for 10 h (×300).

may also be affected to some extent.

3.4. SEM observation of seed coat

The SEM images of the seed coat under each treatment are shown in Fig. 3(a-f). From the observation (Fig. 3a&d), we can see that the surface texture of the seed coat of the normal corn seeds is neat. As for the seed coat with the frozen condition of −10 °C for 10 h (Fig. 3b&e), the surface texture appears occasionally disorderly changes. In the SEM image of the seed coat, 15–35 % of the two/multiple textures are connected to each other, and 10–30 % of the seed coat tissues are uneven. As for the seed coat with the frozen condition of −20 °C for 10 h (Fig. 3c&f), extremely disordered changes in surface texture of corn seed coat. More than 70 % of the texture changes in the seed coat SEM image, not only did more than 30 % of the texture overlap and the unevenness of the seed coat tissue appeared, but also more than 50 % of the texture was unclear and disappeared, and the spacing between two/multiple textures was irregular.

From the results of SEM images, we can know that frostbite has an effect on the surface texture of seed coat. With the deepening of the degree of freezing injury, the seed coat is uneven, the parallelism among the textures is reduced, and the fractures appeared. For the seed coat with the frozen condition of −20 °C for 10 h, more than 70 % of texture change.

3.5. TEM observation of embryo

The TEM images of seed embryo cell under each treatment are shown in Fig. 4(a-i). From the observation (Fig. 4a&d), we can see that the structure of cell membrane, cell wall and cell nucleus of normal seed embryo is intact. As for the seed embryo with the frozen condition of −10 °C for 10 h, the cell structure is partially ruptured (Fig. 4b&e&h): Part of the cell membrane and cell wall have plasmic wall separation, or the definition of the contour between the cell tissue and the cell wall is reduced (Fig. 4b), or the phospholipid molecules in the cell are arranged more spaced, causing 15–30 % of the number to be missing (Fig. 4h), and only 70 %- 85 % of the integrity structure of the nucleus remains (Fig. 4e). The changes are mainly reflected in the distortion of the nuclear membrane part of the nucleus, and a 10–30 % reduction in the content of nucleus. As for the seed embryo with the frozen condition of −20 °C for 10 h, most of the cell structure is broken or cracked (Fig. 4c&f&i): The cell membrane and the cell wall structure are severely separated, the contour between the cell tissue and the cell wall is blurred (Fig. 4c), or more than 70 % of the phospholipid molecules in the cell are missing (Fig. 4i), and the integrity of the nucleus is less than 30 %, the nuclear membrane disappears and more than 70 % of the nucleus is cracked (Fig. 4f).

Through the results of the TEM images, we can know that frostbite has a great influence on the cell structure of seed embryos. The lower the freezing temperature, the more severe the influence on the integrity of the cell structure, the more serious the separation of the cytoplasmic wall, the worse the integrity of the cells and the nucleus. For the seed embryo with the frozen condition of −20 °C for 10 h, the nuclear membrane disappears and more than 70 % of the nucleus is cracked. When the frozen seed is planted, the seed embryo cells cannot absorb nutrients like normal seed cells, so that the seeds cannot grow normally.

The SEM and TEM results obtained in this study are similar to the study by Zheng (2010), which show that slight freezing damage will not cause obvious changes in the appearance of corn seeds. When the water content of the seed is above 20 %, lower temperature will lead to the separation of the pericarp of the seed embryo. Low temperature freezing damage destroyed the normal structure of maize scutellum cells. The osmotic regulation function of the cytoplasmic membrane is unbalanced, part of the cytosol is filled between the cell membrane and the cell wall, and the ridge structure inside the mitochondria is blurred. With the lower of the temperature, the cytoplasmic membrane is damaged, the osmotic regulation function is lost, and a large amount of cytosol is filled between the cell membrane and the cell wall, and some organelle remnants penetrate into the intercellular space. From the study of DeVries et al. (2007), freezing damage of plants is caused by ice crystals formed at low temperature causing damage to cells, and intercellular freezing causes severe dehydration of plant protoplasm, protein denaturation or irreversible gelation of protoplasm. If the temperature of frozen plants suddenly rises, the ice crystals will melt rapidly, and the

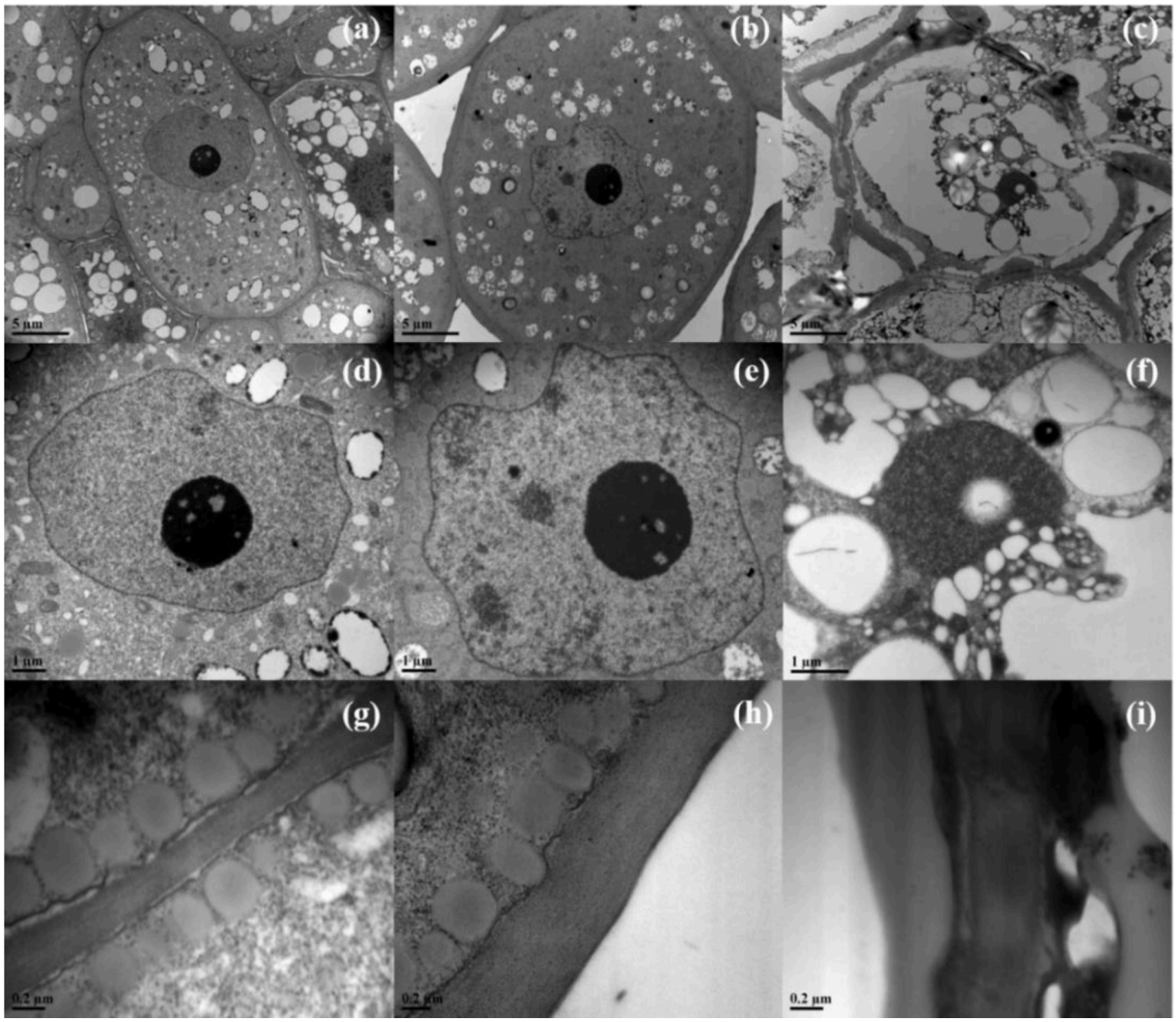

Fig. 4. The TEM images of seed embryo cell under each treatment. (a) the cell structure of normal seeds (×5000); (b) the cell structure of seeds with −10 °C for 10 h (×5000); (c) the cell structure of seeds with −20 °C for 10 h (×6000); (d) the cell nuclear structure of normal seeds (×15000); (e) the cell nuclear structure of seeds with −10 °C for 10 h (×15000); (f) the cell nuclear structure of seeds with −20 °C for 10 h (×25000); (g) the phospholipid molecules of normal seeds (×70000); (h) the phospholipid molecules of seeds with −10 °C for 10 h (×60000); (i) the phospholipid molecules of seeds with −20 °C for 10 h (×70000).

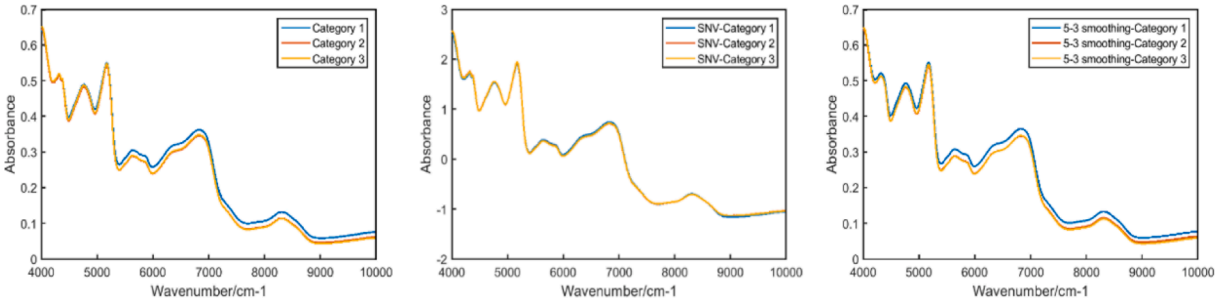

Fig. B1. The average spectra of the corn seeds in the wavenumber range of 400–10000 cm^{-1} under each treatment with (a) none, (b) SNV and (c) 5–3 smoothing pretreatments.

protoplasm will be torn and damaged before it can absorb water. The intracellular freezing will damage the plasma membrane, organelles and the entire cell, causing fatal damage to the plant. The damage caused by these physical changes, chemical changes, physiological changes and mechanical stress inside seeds is irreversible. This may be one of the reasons for the decrease in germination rate of corn seeds after freezing damage (DeVries et al., 2007).

3.6. Results of data processing

3.6.1. Raw and pretreated spectra

Fig. B.1 shows the average spectra of the corn seeds in the wavenumber range of 400–10000 cm^{-1} under three different conditions with none, SNV and 5–3 smoothing pretreatments. From Fig. B.1, it can be seen that the corresponding spectral curve of each freezing condition at

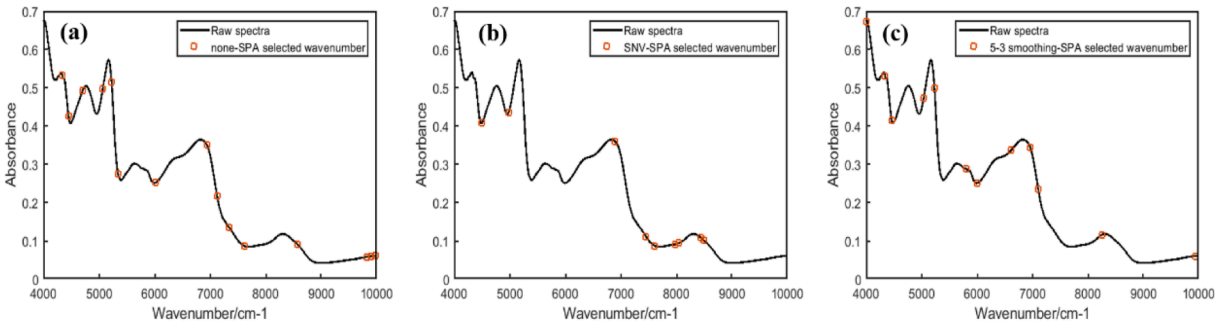

Fig. B2. The position of the selected wavenumbers by SPA method with (a) none, (b) SNV and (c) 5–3 smoothing pretreatments.

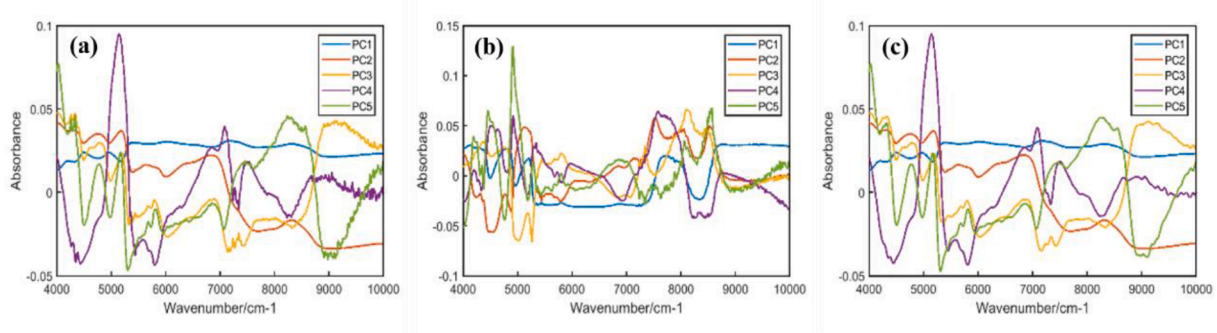

Fig. B3. The first 5 principal components by PCA method with (a) none, (b) SNV and (c) 5–3 smoothing pretreatments.

Table 1
The classification results of KNN and SVM models.

Pretreatments	Feature extraction methods	Models	Training set	Testing set
none	Full wavenumber	KNN	91.7 %	100 %
		SVM	68.3 %	73.3 %
	SPA	KNN	92.8 %	100 %
		SVM	66.1 %	71.1 %
	PCA	KNN	**95.0 %**	**100 %**
		SVM	67.8 %	76.7 %
SNV	Full wavenumber	KNN	96.7 %	100 %
		SVM	80.6 %	82.2 %
	SPA	KNN	96.7 %	100 %
		SVM	81.7 %	82.2 %
	PCA	KNN	**99.4 %**	**100 %**
		SVM	80.0 %	81.1 %
5–3 smoothing	Full wavenumber	KNN	**92.2 %**	**100 %**
		SVM	68.9 %	73.3 %
	SPA	KNN	91.7 %	100 %
		SVM	68.9 %	77.8 %
	PCA	KNN	91.7 %	100 %
		SVM	71.1 %	76.7 %

SNV (standard normal variation) and 5–3 smoothing (five points and three times smoothing) are pretreatment methods; SPA (successive projection algorithm) and PCA (principal component analysis) are feature extraction methods; KNN (K-nearest neighbor) and SVM (support vector machine) are modeling method.

none and 5–3 smoothing pretreatments are extremely similar, the spectral curves of the three freezing conditions under SNV pretreatment are almost overlapped, which may be because the principles of data preprocessing are different. The spectral value at normal condition (category 1) under none and 5–3 smoothing pretreatments in the range of 5200–10000 cm^{-1} is higher than the values at the other two conditions. The spectral curves at −10 °C, 10 h (category 2) and −20 °C,10 h (category 3) conditions are the closest. As the description of Zhang et al in 2021, the reason for this may be the frozen environment. From micro-observation results, the cell structure of the seed was changed and the chemical component of the seed was also changed. The existence of these similarities and differences suggested that different freeze-damages corn seeds were possible to be classified using near-infrared spectral technology.

3.6.2. *Feature wavenumbers*

The feature wavenumbers extracted by SPA and PCA method are shown in Table A.3. It can be seen that less than 15 wavenumbers were selected by SPA method from 1501 wavenumbers for classification, only 12, 9 and 13 feature wavenumbers were obtained under none, SNV and 5–3 smoothing pretreatments respectively. Less than 30 wavenumbers were selected by PCA method from 1501 wavenumbers, only 21, 24 and 26 feature wavenumbers were obtained by PCA method under none, SNV and 5–3 smoothing pretreatments respectively. The number of feature wavenumbers is drastically reduced. Fig. B.2 is the position of the selected wavenumbers by SPA method, and Fig. B.3 is the first 5 principal components by PCA method.

3.6.3. *Classification results*

After the feature wavenumbers were selected, the next step was the classification of spectral data. Table 1 shows the classification accuracy results by KNN and SVM models in both the training and test sets. As shown in Table 1, the modeling performance of KNN model is better than SVM model. The accuracy results obtained by KNN model are all higher than 90 %, while the accuracy results obtained by SVM model are all lower than 85 %. The accuracy result has a great relationship with the modeling principles of the two modeling methods.

Compared the accuracy results among these pretreatments, it can be seen that the accuracy results obtained under SNV pretreatment are higher than those after none and 5–3 smoothing pretreatments, and the performance among none and 5–3 smoothing pretreatment is similar.

Table 2
The confusion matrix of the optimal result in each pretreatment.

Methods		Training set			Testing set		
		Normal	-10°C,10h	-20°C,10h	Normal	-10°C,10h	-20°C,10h
None-PCA-KNN	Normal	59	1	\	30	\	\
	-10°C,10h	1	55	3	\	30	\
	-20°C,10h	\	4	57	\	\	30
	Accuracy,%		95.0%			100%	
SNV-PCA-KNN	Normal	60	\	\	30	\	\
	-10°C,10h	\	59	\	\	30	\
	-20°C,10h	\	1	60	\	\	30
	Accuracy,%		99.4%			100%	
5-3 smoothing-full wavenumber-KNN	Normal	58	3		30	\	\
	-10°C,10h	2	53	5	\	30	\
	-20°C,10h	\	4	55	\	\	30
	Accuracy,%		92.2%			100%	

SNV (standard normal variation) and 5–3 smoothing (five points and three times smoothing) are pretreatment methods; SPA (successive projection algorithm) and PCA (principal component analysis) are feature extraction methods; KNN (K-nearest neighbor) and SVM (support vector machine) are modeling method.

The accuracy result obtained under the SNV pretreatment is increased by at least 4 % compared with the result obtained under none pretreatment, and can be increased by at most 15.6 % in SPA feature extraction method and SVM model. In the case of none pretreatment, the highest accuracy result is obtained in PCA feature extraction method and KNN model with the accuracy of 95.0 % and 100 % for training and testing set. In the case of SNV pretreatment, the highest accuracy result is obtained in PCA feature extraction method and KNN model with the accuracy of 99.4 % and 100 % for training and testing set, and for 5–3 smoothing pretreatment, the highest accuracy result is obtained in full wavenumber method and KNN model with the accuracy of 92.2 % and 100 % for training and testing set.

In the case of feature extraction methods, the performance of the three feature extraction methods is ordered as PCA method > SPA method > full wavenumber method. In the case of SNV pretreatment and KNN model, PCA feature extraction method obtained 99.4 % and 100 % accuracy result, while both full number feature extraction method and SPA feature extraction method obtained 96.7 % and 100 % accuracy result for training and testing set. In the case of none pretreatments, the best accuracy results are obtained after the features are extracted by PCA method. It shows that the use of the feature extraction method not only saves the modeling time, but also obtains better modeling results to a certain extent compared with using the full wavenumbers.

The confusion matrix of the optimal result in each pretreatment is shown in Table 2. It can be seen that classification errors mainly occur in the freezing conditions of −10 °C, 10 h and −20 °C, 10 h. This can be confirmed from the spectra curves of the seeds. The spectra under the two conditions (−10 °C, 10 h and −20 °C, 10 h) are very close, and the degree of coincidence is high. The spectral value of the seed under normal conditions is relatively higher than the values under freezing conditions, thus there is spectral difference appeared. Of course, there are also misclassifications between normal and −10 °C, 10 h. It also can be seen that the data of the testing set under different freezing conditions were not misclassified during classification, indicating that the methods have the advantage of obtaining wonderful classification results.

Other studies focused on the research of frozen corn seeds were compared. Although the studies of Woltz et al. have explored the influencing factors (corn seed maturity, moisture content, freezing temperature and duration) of seed frostbite, how frostbite affects the growth and development of corn seeds was not explored (Woltz, Egli & TeKrony, 2005; Woltz, TeKrony & Egli, 2006). In addition, no detection technology was introduced.

In the study of Jia et al (2016), the authors classified corn seeds into two categories, and a highest 97 % average accuracy was obtained. Through comparison and analysis, the seeds used in the study had large vigor difference. One category seeds were normal seeds without freezing damage, and another category seeds with low vigor under severe frozen condition (the original moisture content is 30 %, and the frostbite temperature is −19.2 °C), thus it's easy to classify the seeds (Jia, et al., 2016). In addition, the influence of frostbite on the main parts of seeds was not explored. Compared with above study, we first explored the germination condition and biological indicators changes of freezing damaged corn seeds, and then explored the influence of frostbite on the main parts of seeds from the microscopic level, and finally a good classification of three categories of freezing-damaged seeds was achieved by using near-infrared technology.

4. Conclusions

Different freezing-damaged corn seeds were prepared after placed in different frozen conditions. The germination and growth of corn seeds, the activities of related enzymes (SOD, POD, CAT, AMS) under different freezing conditions reflect the effect of frostbite on corn seeds. With the deeper the degree of frostbite, the lower the germination rate of corn seeds. On day 7, the germination of seeds in each treatment has

increased, and the germination rate of seeds under the frozen condition of normal, −10 °C for10h and −20 °C for 10 h are 88 %, 42 % and 10 % respectively. From the SEM and TEM observations, the texture of the seed coat and the cell structure of the seed embryo were affected to varying degrees with the degree of frostbite. For the seed coat and seed embryo with the frozen condition of −20 °C for 10 h, more than 70 % of texture change and most of the cell structure is broken or cracked, the nuclear membrane disappears and more than 70 % of the nucleus is cracked. The micro-observation result confirmed that frostbite had an adverse effect on corn seeds, which providing theoretical support for the subsequent use of near-infrared spectroscopy to realize the classification of corn seeds. Finally, in the case of SNV pretreatment–PCA feature extraction method-KNN model, 99.4 % and 100 % classification results of the training set and testing set were obtained respectively.

CRediT authorship contribution statement

Jun Zhang: Conceptualization, Data curation, Methodology, Investigation, Writing – original draft. **Zhiying Wang:** Data curation, Writing – review & editing. **Maozhen Qu:** Data curation, Writing – review & editing. **Fang Cheng:** Conceptualization, Funding acquisition, Supervision, Writing – review & editing.

Declaration of Competing Interest

The authors declare that they have no known competing financial interests or personal relationships that could have appeared to influence the work reported in this paper.

Acknowledgments

The authors are grateful for the Gansu Dunhuang Seed Group Co., Ltd for providing the corn seeds. This work was financially supported by the National Natural Science Foundation of China (Grant No. 61873231).

Appendix

Table A1
The germination results of the corn seeds on Day 4 and Day 7 of each treatment.

Treatment	Germination rate on Day 4 (%)	Germination rate on Day 7 (%)
Normal	70	88
−10 °C,10 h	28	42
−20 °C,10 h	6	10

Table A2
The enzyme activity results of SOD, POD, CAT and AMS under each treatment.

Treatment	SOD activity (U/g)	POD activity (U/g)	CAT activity (U/g)	AMS activity (U/g)
Normal	981.492 ± 4.727c	50.370 ± 4.207 ab	19.507 ± 2.383c	1.310 ± 0.108c
−10 °C,10 h	1358.467 ± 27.747 a	57.407 ± 2.313 a	29.849 ± 6.531b	2.466 ± 0.175 a
−20 °C,10 h	1222.839 ± 100.919b	41.852 ± 7.229b	41.474 ± 1.076 a	1.936 ± 0.057b

Results are expressed as mean ± SD (standard deviation) of three determinations. The different letters within the same indicator indicate a significant difference between the freezing conditions (p less than 0.05).

Table A3
The selected wavenumbers by feature extraction methods in different pretreatments.

Pretreatments	Feature extraction method	Number of wavenumbers	Wavenumbers /cm^{-1}
None	full wavenumber	1501	10000–4000
	SPA	12	4008 4256 4852 5152 5344 5792 6252 6896 7128 7344 7636 8236
	PCA	21	4328 4428 4500 4748 4968 5136 5172 5208 5308 5400 5636 5792 6000 6884 7084 7168 7344 7504 8232 8340 9116
SNV	full wavenumber	1501	10000–4000
	SPA	9	4500 4984 6896 7456 7612 7980 8048 8444 8496
	PCA	24	4184 4364 4452 4492 4772 4912 4948 5012 5124 5208 5260 5340 5792 6924 7076 7344 7524 7580 7684 8096 8344 8452 8520 8720
5–3 smoothing	full wavenumber	1501	10000–4000
	SPA	13	4028 4256 5120 5808 6268 6972 7124 7632 8100 8400 9880 9932 10,000
	PCA	26	4332 4444 4484 4504 4756 4952 4996 5140 5168 5316 5392 5636 5800 5996 6024 6848 6900 7160 7424 7504 8256 8312 8668 8868 9108 9132

SNV (standard normal variation) and 5–3 smoothing (five points and three times smoothing) are pretreatment methods; SPA (successive projection algorithm) and PCA (principal component analysis) are feature extraction methods; KNN (K-nearest neighbor) and SVM (support vector machine) are modeling method.

References

Akinyosoye, S. T., Adetumbi, J. A., Amusa, O. D., Olowolafe, M. O., & Olasoji, J. O. (2014). Effect of seed size on in vitro seed germination, seedling growth, embryogenic callus induction and plantlet regeneration from embryo of maize (*Zea mays* L.) seed. *Nigerian. Journal of Genetics, 28*(2), 1–7. https://doi.org/10.1016/j.nigjg.2015.06.001

Ambrose, A., Kandpal, L. M., Kim, M. S., Lee, W., & Cho, B. (2016). High speed measurement of corn seed viability using hyperspectral imaging. *Infrared Physics & Technology, 75*, 173–179. https://doi.org/10.1016/j.infrared.2015.12.008

Armstrong, P. R. (2007). The effect of moisture content on determining corn hardness from grinding time, grinding energy, and near-infrared spectroscopy. *Applied Engineering in Agriculture, 23*(6), 793–799. https://doi.org/10.13031/2013.24046

Burges, C. J. C. (1998). A tutorial on support vector machines for pattern recognition. *Data Mining and Knowledge Discovery, 2*(2), 121–167. https://doi.org/10.1023/A:1009715923555

Candolfi, A., De Maesschalck, R., Jouan-Rimbaud, D., Hailey, P. A., & Massart, D. L. (1999). The influence of data pre-processing in the pattern recognition of excipients near-infrared spectra. *Journal of Pharmaceutical and Biomedical Analysis, 21*(1), 115–132. https://doi.org/10.1016/S0731-7085(99)00125-9

Chen, H., Song, Q., Tang, G., Feng, Q., & Lin, L. (2013). The combined optimization of savitzky-golay smoothing and multiplicative scatter correction for FT-NIR PLS models. *ISRN Spectroscopy, 2013*, 1–9. https://doi.org/10.1155/2013/642190

Cui, Y., Xu, L., An, D., Liu, Z., Gu, J., Li, S., Zhang, X., & Zhu, D. (2018). Identification of maize seed varieties based on near infrared reflectance spectroscopy and chemometrics. *International Journal of Agricultural and Biological Engineering, 11*(2), 177–183. https://doi.org/10.25165/j.ijabe.20181102.2815

Da Conceição, R. R. P., Simeone, M. L. F., Queiroz, V. A. V., de Medeiros, E. P., de Araújo, J. B., Coutinho, W. M., … de Resende Stoianoff, M. A. (2021). Application of near-infrared hyperspectral (NIR) images combined with multivariate image analysis in the differentiation of two mycotoxicogenic Fusarium species associated with maize. *Food Chemistry, 344*, Article 128615. https://doi.org/10.1016/j.foodchem.2020.128615

de Sousa Fernandes, D. D., de Almeida, V. E., Fontes, M. M., de Araújo, M. C. U., Véras, G., & Diniz, P. H. G. D. (2019). Simultaneous identification of the wood types in aged cachaças and their adulterations with wood extracts using digital images and SPA-LDA. *Food Chemistry, 273*, 77–84. https://doi.org/10.1016/j.foodchem.2018.02.035

DeVries, M., Goggi, A. S., & Moore, K. J. (2007). Determining seed performance of frost-damaged maize seed lots. *Crop Science, 47*(5), 2089–2097. https://doi.org/10.2135/cropsci2007.01.0005

Egesel, C.Ö., Kahrıman, F., Ekinci, N., Kavdır, O., & Büyükcan, M. B. (2016). Analysis of fatty acids in kernel, flour, and oil samples of maize by NIR spectroscopy using conventional regression methods. *Cereal Chemistry Journal, 93*(5), 487–492. https://doi.org/10.1094/CCHEM-12-15-0247-R

Gratão, P. L., Polle, A., Lea, P. J., & Azevedo, R. A. (2005). Making the life of heavy metal-stressed plants a little easier. *Functional Plant Biology, 32*(6), 481. https://doi.org/10.1071/FP05016

Gustin, J. L., Jackson, S., Williams, C., Patel, A., Armstrong, P., Peter, G. F., & Settles, A. M. (2013). Analysis of maize (*Zea mays*) kernel density and volume using microcomputed tomography and single-kernel near-infrared spectroscopy. *Journal of Agricultural and Food Chemistry, 61*(46), 10872–10880. https://doi.org/10.1021/jf403790v

Jia, S., Yang, L., An, D., Liu, Z., Yan, Y., Li, S., … Gu, J. (2016). Feasibility of analyzing frost-damaged and non-viable maize kernels based on near infrared spectroscopy and chemometrics. *Journal of Cereal Science, 69*, 145–150. https://doi.org/10.1016/j.jcs.2016.02.018

Li, H. X., Xiao, Y., Cao, L. L., Yan, X., Li, C., Shi, H. Y., … Ye, Y. H. (2013). Cerebroside C increases tolerance to chilling injury and alters lipid composition in wheat roots. *Plos One, 8*(9), e73380.

Lin, J., Yu, L., Li, W., & Qin, H. (2018). Method for Identifying Maize Haploid Seeds by Applying Diffuse Transmission Near-Infrared Spectroscopy. *Applied Spectroscopy, 72*(4), 611–617. https://doi.org/10.1177/0003702817742790

Lin, Y., He, S., Lu, Z., Gao, Y., Duan, Y., Li, Z., … Gui, F. (2020). Influence of Aphis gossypii feeding on defense strategy of native and introduced populations of Ageratina adenophora. *Arthropod-Plant Interactions, 14*(3), 345–356. https://doi.org/10.1007/s11829-020-09748-7

Liu, D., Sun, D., & Zeng, X. (2014). Recent advances in wavelength selection techniques for hyperspectral image processing in the food industry. *Food and Bioprocess Technology, 7*(2), 307–323. https://doi.org/10.1007/s11947-013-1193-6

Liu, X., Zhang, L., Pang, X., Wu, Y., Wu, Y., Shu, Q., … Zhang, X. (2022). Synergistic antibacterial effect and mechanism of high hydrostatic pressure and mannosylerythritol Lipid-A on Listeria monocytogenes. *Food Control, 135*, Article 108797. https://doi.org/10.1016/j.foodcont.2021.108797

Lu, P., Wang, R., Zhu, C., Fu, X., Wang, S., Grierson, D., & Xu, C. (2019). Microscopic analyses of fruit cell plastid development in loquat (Eriobotrya japonica) during Fruit Ripening. *Molecules, 24*(3), 448. https://doi.org/10.3390/molecules24030448

Mavroforakis, M. E., & Theodoridis, S. (2006). A geometric approach to Support Vector Machine (SVM) classification. *IEEE Transactions on Neural Networks, 17*(3), 671–682. https://doi.org/10.1109/TNN.2006.873281

Nan, M. (2010). *Influence of freezing injury on gernination and physiological-biochemical changes in different grain types of maize seed*. Gansu Agricultural University. Dissertation.

Qiao, M., Xu, Y., Xia, G., Su, Y., Lu, B., Gao, X., & Fan, H. (2022). Determination of hardness for maize kernels based on hyperspectral imaging. *Food Chemistry, 366*, Article 130559. https://doi.org/10.1016/j.foodchem.2021.130559

Qiu, G., Lü, E., Lu, H., Xu, S., Zeng, F., & Shui, Q. (2018). Single-Kernel FT-NIR Spectroscopy for Detecting Supersweet Corn (Zea mays L. Saccharata Sturt) Seed Viability with Multivariate Data Analysis. *Sensors, 18*(4), 1010. https://doi.org/10.3390/s18041010

Rajput, I. R., Li, Y. L., Xu, X., Huang, Y., Zhi, W. C., Yu, D. Y., & Li, W. (2013). Supplementary Effects of Saccharomyces boulardii and Bacillus subtilis B10 on Digestive Enzyme Activities, Antioxidation Capacity and Blood Homeostasis in Broiler. *International Journal of Agriculture and Biology, 15*(2).

Riba Ruiz, J., Canals, T., & Cantero Gomez, R. (2012). Comparative study of multivariate methods to identify paper finishes using infrared spectroscopy. *IEEE Transactions on Instrumentation and Measurement, 61*(4), 1029–1036. https://doi.org/10.1109/TIM.2011.2173048

Santos, M. C. D., Morais, C. L. M., Nascimento, Y. M., Araujo, J. M. G., & Lima, K. M. G. (2017). Spectroscopy with computational analysis in virological studies: A decade (2006–2016). *TrAC Trends in Analytical Chemistry, 97*, 244–256. https://doi.org/10.1016/j.trac.2017.09.015

Soares, S. F. C., Gomes, A. A., Araujo, M. C. U., Filho, A. R. G., & Galvão, R. K. H. (2013). The successive projections algorithm. *TrAC Trends in Analytical Chemistry, 42*, 84–98. https://doi.org/10.1016/j.trac.2012.09.006

Sun, R., Zhou, Q., Sun, F., & Jin, C. (2007). Antioxidative defense and proline/phytochelatin accumulation in a newly discovered Cd-hyperaccumulator, Solanum nigrum L. *Environmental and Experimental Botany, 60*(3), 468–476. https://doi.org/10.1016/j.envexpbot.2007.01.004

Wold, S., Esbensen, K., & Geladi, P. (1987). Principal component analysis. *Chemometrics and Intelligent Laboratory Systems, 2*(1–3), 37–52. https://doi.org/10.1016/0169-7439(87)80084-9

Woltz, J. M., Egli, D. B., & TeKrony, D. M. (2005). Freezing Point Temperatures of Corn Seed Structures during Seed Development. *Agronomy Journal, 97*(6), 1564–1569. https://doi.org/10.2134/agronj2005.0073

Woltz, J., TeKrony, D. M., & Egli, D. B. (2006). Corn Seed Germination and Vigor Following Freezing during Seed Development. *Crop Science, 46*(4), 1526–1535. https://doi.org/10.2135/cropsci2005.08-0292

Yang, X., Hong, H., You, Z., & Cheng, F. (2015). Spectral and image integrated analysis of hyperspectral data for waxy corn seed variety classification. *Sensors, 15*(7), 15578–15594. https://doi.org/10.3390/s150715578

Zhang, J., Dai, L., & Cheng, F. (2019). Classification of frozen corn seeds using hyperspectral VIS/NIR reflectance imaging. *Molecules, 24*(1), 149. https://doi.org/10.3390/molecules24010149

Zhang, J., Dai, L., & Cheng, F. (2021a). Identification of Corn Seeds with Different Freezing Damage Degree Based on Hyperspectral Reflectance Imaging and Deep Learning Method. *Food Analytical Methods, 14*(2), 389–400. https://doi.org/10.1007/s12161-020-01871-8

Zhang, J., Dai, L., & Cheng, F. (2021b). Corn seed variety classification based on hyperspectral reflectance imaging and deep convolutional neural network. *Journal of Food Measurement and Characterization, 15*(1), 484–494. https://doi.org/10.1007/s11694-020-00646-3

Zheng, Q. (2010). *Influence of freezing injury on germination characteristics and structure of hybrid maize seed*. Gansu Agricultural University. Dissertation.

Zhong, J., & Qin, X. (2016). Rapid quantitative analysis of corn starch adulteration in konjac glucomannan by chemometrics-assisted FT-NIR spectroscopy. *Food Analytical Methods, 9*(1), 61–67. https://doi.org/10.1007/s12161-015-0176-9